DIELECTRIC PASSIVATION SCHEMES FOR HIGH EFFICIENCY N-TYPE C-SI SOLAR CELLS

D.S. Saynova[1], I.G. Romijn[1*], I. Cesar[1], M.W.P.E. Lamers[1], A. Gutjahr[1], G. Dingemans[2]
H.C.M. Knoops[3], B.W.H. van de Loo[3], W.M.M. Kessels[3], O. Siarheyeva[4], E. Granneman[4], L. Gautero[5], D.M. Borsa[5],
P.R. Venema[6], A.H.G. Vlooswijk[6]
[1]ECN Solar Energy, P.O. Box 1, NL-1755 ZG Petten, the Netherlands
Phone: +31 224 56 4309; Fax: +31 224 56 8214; email: romijn@ecn.nl
[2]ASM, Kapeldreef 75, B-3001 Leuven, Belgium,
[3]Eindhoven University of Technology, Department of Appl. Physics, P.O. Box 513, 5600 MB Eindhoven, NL
[4]Levitech BV, Versterkerstraat 10, 1322AP Almere, The Netherlands, 5Roth & Rau B.V. Luchthavenweg 10, 5657 EB
Eindhoven, NL
[6]Tempress Systems BV, Radeweg 31, 8171 Vaassen, NL

ABSTRACT: We investigate the impact of different dielectric layers and stacks on the passivation properties of boron doped p^{++}-emitters and phosphorous doped n^+-BSFs which are relevant for competitive n-type cell conversion efficiencies. The applied passivation schemes are associated with specific properties at c-Si/dielectric interface and functional mechanisms. In this way we aim to gain a deeper understanding of the passivation mechanism of the differently doped fields within the n-type cells and identify options to further improve the efficiency. The deposition technologies in our study comprise industrial PECVD systems and/or ALD both in industrial and lab scale configurations. In case of p^{++}-emitters the best results were achieved by combining field effect and chemical passivation using stacks of low temperature wet chemical oxide and thin ALD-AlOx capped with PECVD-SiNx. The corresponding Implied Voc values were of about (673 ± 2) mV and J_0 of (68 ± 2) fA/cm^2. For the n^+-BSF passivation the passivation scheme based on SiOx with or without additional AlOx film deposited by a lab scale temporal ALD processes and capped with PECVD-SiNx layer yielded a comparable Implied Voc of (673 ± 2) mV, but then corresponding to J_0 value of (80 ± 15) fA/cm^2. This passivation scheme is mainly based on the chemical passivation and was also suitable for p++ surface. This means that we have demonstrated that for n-Pasha cells both the emitter and BSF can be passivated with the same type of passivation that should lead to > 20% cell efficiency. This offers the possibility for transfer this passivation scheme to advanced cell architectures, such as IBC.
Keywords: passivation, n-type, boron emitter, back-surface-field

1 INTRODUCTION

The importance of n-type *c*-Si material for PV applications has been emphasized by the International Technology Roadmap for Photovoltaics[1]. In particular, n-type mono-Si material currently results in significantly higher efficiency potential for c-Si solar cells, i.e at least 0.5% absolute difference in stabilized efficiency compared to p-type mono material. In this way n-type mono-Si material is highly relevant for advanced cell technologies such as IBC, HJ and bifacial configurations..

In 2010, ECN, Tempress and Yingli introduced the n-Pasha cell to the market as a novel bifacial cell concept based on n-type Cz material with homogeneous diffusions, dielectric passivation and printed metallization [2, 3]. A major R&D topic ever since has been the conversion efficiency improvement, which has been recognized as one of the major drivers for reduced cost of c-Si modules[4]. An important strategy in this respect is the reduction in the recombination losses associated with the emitter and BSF [5]. The implementation of a lightly doped BSF was one of the elements which enabled average efficiencies of 20% and top efficiencies of 20.2% in 2012 for n-Pasha cells [6]. The optimal utilization of high-efficiency emitter and optimized BSF requires effective surface passivation schemes. This aspect becomes increasingly relevant in combination with thin wafers [7] which contribute to optimal silicon utilization and thereby further improve the cost reduction potential of the c-Si modules.

We present an investigation of the passivation impact of different dielectric layers and stacks applied on boron emitters and phosphorous BSFs. The structures are relevant for competitive n-type cell conversion efficiencies. The deposition technologies in our study comprise industrial PECVD systems and/or ALD both in industrial and lab scale configurations.

2 INVESTIGATION APPROACH

The design of the dielectric layers followed two strategies: 1) promotion of both field effect and chemical passivation by choosing a suitable fixed charge at the interface (Q_f) and low density of interface states (D_{it}), as well as 2) maintaining low D_{it} while targeting close to neutral Q_f. The first approach is the typical way to carry out such optimizations. In the second case we follow a novel strategy to achieve functional passivation for both emitter and BSF at the same time. In this way the applications can be extended also to advanced cell architectures, such as IBC. In view of the intended applications in solar cell process involving a firing step, the high temperature stability was an important aspect of the characterization. Several types of passivation schemes were included in the study:

- Dielectric stack SiOx/PECVD-SiNx
  By applying different types of SiOx layers at the Si interface, the passivation mechanism is either based on predominantly chemical passivation, applicable to both p^{++}-emitter and n^+-BSF, or combines chemical and field effect components. The latter is expected to be most suitable for n^+-BSF passivation due to the positive Q_f. The SiOx layer in the stack was processed using low temperature ($\leq$ 200°C) (LT) techniques such as ETP-PECVD, growth from a wet chemical solution (NAOS), or a temporal, low pressure ALD process in a single wafer tool (SW-ALD) were used [8]. NAOS/SiN$_x$ passivation was reported to be very effective for passivation of front side boron emitters [9] and we extend application

to phosphorous BSF.

- NAOS/ALD-AlOx/PECVD-SiNx
  This group represents a variation to ALD-AlOx/SiNx dielectric stacks that have been widely used for passivation of boron emitters with various doping profiles for cell applications [10-12]. The success of this passivation scheme is attributed to the combination of chemical and field effect passivation by negative fixed charges [13, 14]. For the current study novel HVM tools for Al2O3 deposition were used. Two different industrial ALD systems were employed: low pressure ALD batch system (batch-ALD) as well as spatial atmospheric pressure ALD (spatial-ALD).
- ALD-SiOx/ALD-AlOx/PECVD-SiNx
  The SiOx was deposited by SW-ALD and subsequently capped with AlOx deposited by the same method. This particular scheme is specially designed to passivate both p^{++}-emitter and n^{+}-BSF simultaneously. Studies on lightly doped p- or n-type polished substrates showed that the presence of AlOx improved the D_{it}, compared to the single ALD-SiOx layer [15]. In addition, the chosen SiOx film-thickness of 3nm, results in a strong reduction of the negative Q_f associated with ALD AlOx layer [8]. In the current study we transfer this approach from lightly doped and polished Si substrates to highly doped p^{+}- and n^{+}- textured surfaces and add SiNx capping to obtain structures directly applicable to c-Si solar cells.

2 EXPERIMENTAL DETAILS

Industrially grown n-CZ material of resistivity 11.8 or 10.2 Ohm.cm was used for the sample preparation with configuration $p^{++}/n/p^{++}$ or $p^{++}/n/n^{+}$, respectively. Schematic cross sections of the two layouts are shown in Figure 1a) and b). The symmetrical samples correspond to the boron emitter passivation studies. The asymmetrical layout was applied for BSF-part of the investigation. The sample-preparation comprised an industrial random pyramid (RP) wafer texture, followed by a diffusion of the boron emitter and BSF using BBr3 or POCl3 tube furnace processes. After glass removal and cleaning steps, several passivation schemes were applied based on the layers listed in Table I. Finally the samples were fired at temperature settings typical for high efficiency n-Pasha cell preparation. It should be noted that the sample preparation was successfully carried out in collaboration between different scientific institutions and/or industrial partners. In this respect following an explicitly scheduled deposition timescale was of vital importance.

Table I: Dielectric layers included in various passivation schemes

Layer	Deposition process
AlOx1	Batch-ALD (temporal, low pressure ALD, batch system)
AlOx2	Spatial-ALD (spatial, atmospheric pressure ALD)
AlOx3	SW-ALD (temporal, low pressure ALD, single wafer system)
SiOx1	SW-ALD (temporal, low pressure ALD, single wafer system)

Layer	Deposition process
SiOx2	ETP PECVD
SiNx1 & 2	Remote PECVD
SiNx3	Direct PECVD

The functionality of the different passivation schemes was monitored by QSSPC-method and WCT-120: Silicon Wafer Lifetime Tester from Sinton Instruments [16]. The Implied Voc (iVoc) values were measured at 1 sun. In addition J_0/side was evaluated at high injection level regime (> 5 suns) [17]. The J_0/side values measured for the different passivation schemes in general follow the trend of the Implied Voc results. The samples in the J_0 case are probed at high injection level and therefore some variation with respect to the performance at 1 sun can be expected.

(a)

(b)
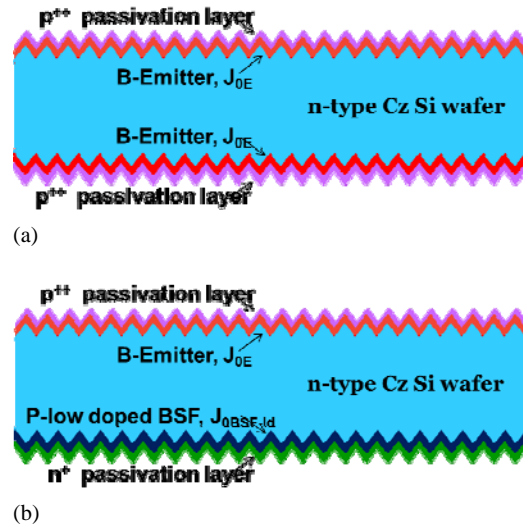
Figure 1: Schematic cross section of the sample layout: (a) symmetrical type $p^{++}/n/p^{++}$, (b) asymmetrical samples $p^{++}/n/n^{+}$. The wafers were textured on both sides

3 RESULTS AND DISCUSSION

3.1 Passivation of boron-diffused emitter

An overview of the iVoc and J_0/side results measured for the different passivation schemes applied on boron emitters is shown in Figure 2 (a) and (b), respectively. The layer deposition was accomplished using various industrial scale equipments, with the exception of the two groups containing SiOx1 and/or AlOx3 films (see also Table I). The data are displayed as mean values with error bars corresponding to the 95% Tukey honest significant difference (HSD) intervals. In order to probe the relevance of the results for industrial solar cell processes which include a screen printing/firing step, the low temperature dielectric layers were kept at thickness $\leq$ 5 nm and the sample measurements were performed after firing. The target value of 660 mV for iVoc that enables achievement of $\geq$ 20 % n-Pasha cell efficiency is also shown. After metallization, the values obtained for Voc are typically ~10 mV lower compared to i-Voc, as will be discussed later in this paper.
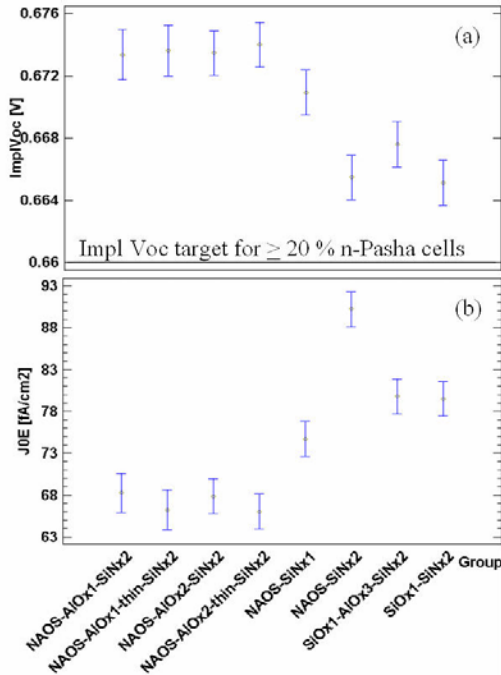
Figure 2: Passivation results for boron-diffused emitter: (a) ImplVoc at 1 Sun, (b) J_0/side at 5 Suns illumination

The data summarized in Figure 2 demonstrate compatibility of the different tested boron emitter passivation schemes with cell efficiencies $\geq$ 20 %.

The highest Implied Voc values of ~(673$\pm$2) mV were achieved for the passivation with NAOS/ALD-AlOx layers capped with PECVD-SiNx (Figure 2a). AlOx layers were deposited using two different industrial ALD systems: batch or spatial industrial ALD. It should be noted that for both techniques the passivation remained stable when the AlOx layer thickness in the stacks was reduced to 2 nm (AlOx-thin in figure 2). The successful performance of this passivation scheme can be understood in terms of combined chemical and field effect passivation due to the negative fixed charge of the AlOx layer. The result is in line with publications of other authors, although in previous studies no NAOS and usually thicker Al2O3 layers were used [11, 12, 18]. Unlike the previous reports, in our case in order to facilitate industrial transfer, we successfully combine textured surfaces with thin AlOx layers and activate the passivation only by the thermal budget from the PECVD SiN deposition and the firing process. We observed no variation in the results corresponding to the deposition tool applied. As the Implied Voc values are higher than 670 mV it is likely that the implied Voc is mainly limited by emitter (Auger) and/or bulk recombination. Both options are plausible, as we are using relatively low R_{sheet} of the boron emitter (60 ohm/sq, as shown in Table II below) in combination with Cz material [19]. Currently corona-charge measurements are on-going to identify these limiting mechanisms.

Preliminary corona-charge measurements suggest that the surface is well passivated. In this experiment no further improvement in J_0 was observed when depositing negative corona charges, while for depositing positive corona charges a degradation was observed in line with expected reduced field-effect passivation.

Another successful approach in our study of boron emitter passivation is by using low temperature SiOx layers obtained either by wet chemical or ALD processes. In this case we expect major impact from the chemical passivation at the NAOS/p^{++}-Si or ALD-SiOx/p^{++}-Si interface.

In case of NAOS-interface a significant improvement of the Impl Voc by (6$\pm$2) mV was achieved by tuning the SiNx-layer towards more H-rich SiNx:H compositions. (layers NAOS-SiNx1 vs SiOx1-AlOx3-SiNx2)

The passivation of the scheme based on ALD-SiOx was also improved by including 2 nm AlOx layer deposited in the same ALD tool before the PECVD-SiNx capping (layers SiOx1-AlOx3-SiNx2 vs SiOx1-SiNx2). A slight increase of the Impl Voc was observed for the SiOx-AlOx3-SiNx2 versus the SiOx1-Al2O3 layers (measured at 1 sun), however this was not reflected in the corresponding values for J_{0E} at higher injection levels. The chosen thickness of the ALD-SiOx layer was 3 nm and therefore the total fixed charge of the SiOx1-AlOx3-SiNx2 stack is expected to be close to 0 [8]. The small improvement trend of the passivation in this case can be understood with a more effective hydrogenation of the interface due to the additional H-supply and/or inhibited H-effusion due to the AlOx layer.

Previous studies on lightly n-doped wafers reported the reduction of D_{it} by one order of magnitude to ~ 10^{11} cm^{-2} eV^{-1} when ALD-SiOx films, like SiOx1 in this study, were capped with ALD-AlOx [15]. In the present investigation we have successfully transferred this approach to industrially textured and highly p^{++}-doped surfaces and include PECVD-SiNx capping to achieve test structures that are relevant to solar cells with front side boron emitter and efficiencies > 20%.

The J_0 values are compared to the literature data in Table II. In principle it is difficult to benchmark various reports on different wafers, employing different diffusions and a variation of surface doping levels. Therefore, the results in this paper are highly relevant due to the comparison of different passivation films on the same diffused samples (with same wafer type, surface pre-treatment, surface concentration and sheet resistance). In order to make a more relevant comparison we corrected the J_0 values for the increase in surface area due to texturization. As summarized in Table II several excellent passivation schemes were demonstrated in our study with J_0 values below 50 fA/cm^2 (after correction for the textured surface).

Table II: Comparison of the best achieved emitter saturation current density values with literature data of passivation schemes using similar deposition methods and layer structures.

J_0 [fA/cm^2]	Boron emitter R_{sheet} [Ohm/sq]	Passivation scheme details
10/26	>100/54	Planar surface ALD, 30 nm AlOx Anneal 30 min/425 °C [12]
62	90	Planar surface ALD, 27 nm AlOx After firing 825 °C [11]
38$^{\#}$	87	ALD, 20 nm AlOx + PECVD SiNx Anneal 25 min/450 °C
40$^{\#}$	60	NAOS-AlOx1 and 2-SiNx2

J_0 [fA/cm^2]	Boron emitter R_{sheet} [Ohm/sq]	Passivation scheme details
44[#]	60	NAOS-SiNx2
47[#]	60	SiOx1-(w/w-o)AlOx3-SiNx2

[#]Corrected for surf. texture

In order to link the passivation performance with the resulting cell characteristics, we used model calculations for the Voc and recombination current at the front and rear of the cell [5]. The Voc also depends on the bulk diffusion length. Therefore we included two typical values for the n-base material. The 20% n-Pasha cell results are also shown with Voc of 650 mV [6, 20]. This parameter was used to set the margin for the iVoc at >660 mV, assuming at least 10 mV difference due to contact recombination. The results obtained for the passivation schemes applied on the boron emitters are also included in the graph. A very good agreement is observed between the experimental data and numerical calculations results for higher quality n-type material with diffusion length of 3 mm.
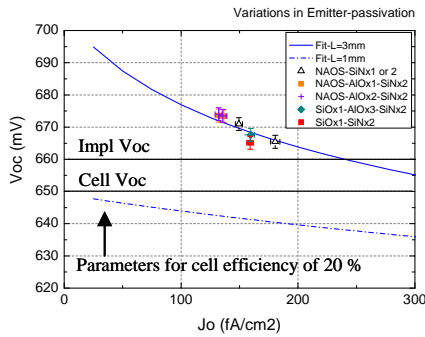
Figure 3: Model calculations of the dependence of Voc on recombination current J_0 for two typical minority carrier diffusion lengths, L in the n-type base of 1 and 3 mm. The experimental results for the boron emitter passivation schemes are also shown in the graph

3.2 Passivation of phosphorous-diffused BSF

Various passivation schemes were also applied to phosphorous-diffused BSF and the resultant performance was evaluated after a firing step. In this study symmetrical p^{++}/n/p^{++} and asymmetrical samples p^{++}/n/n$^+$ were included. The passivation of the p^{++} boron emitters was accomplished by NAOS-SiNx1 stack in all cases. The asymmetric samples comprised relatively low doped phosphorous diffused BSF with R_{sheet} ~40 Ohm/sq and surface doping levels <10^{20} cm^{-3}. As a result the samples were more sensitive to variations in the surface recombination. The J_0 values obtained from the symmetric p^{++}/n/p^{++} samples were used to derive the J_0 of the n/n$^+$ (BSF) side of the asymmetrical p^{++}/n/n$^+$ samples. An overview of the iVoc and J_0/BSF-side values measured for the different passivation schemes is shown in Figure 4 (a) and (b), respectively. The data are displayed as mean values with error bars corresponding to the 95% Tukey HSD intervals. Similar to the boron emitter passivation results discussed in the previous section, most of the utilized deposition systems were industrial scale tools (please see also Table I).
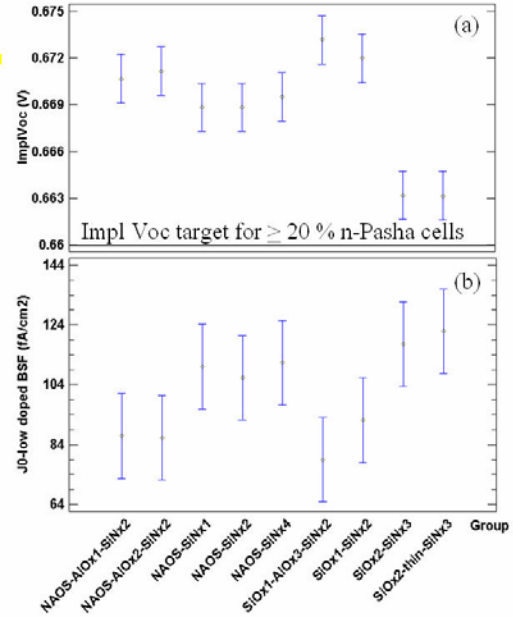
Figure 4: Passivation results for phosphorous-diffused BSF: (a) ImplVoc, (b) J_0/side

As can be seen in Figure 4(a), all tested layers supplied sufficient passivation of the BSF to pass the 660 mV threshold; this means that with all layers, >20% n-Pasha cells can be fabricated. Some differences are still visible for the different layers however.

The layer with neutral fixed charge capped by AlOx - SiOx1-AlOx3-SiNx1 - performs best, iVoc was (673 ± 2) mV corresponding to J_0 value of (80 ± 10) fA/cm^2. In this case the major passivation mechanism relies on reduced D_{it} value. The AlOx layer capping yields an improvement over simply applying ALD SiOx1-SiNx1 layers. As was the case for the p+ emitter passivation, this improvement trend of the passivation can be understood with a more effective hydrogenation of the interface due to the additional H-supply and/or inhibited H-effusion due to the AlOx layer.

Comparable performance was achieved utilizing AlOx layers deposited on n+/NAOS interface by industrial ALD processes (NAOS-AlOx1-SiNx2 and NAOS-AlOx2-SiNx2). The obtained results on textured surface of J_0 values about 85 fA/cm^2 and ImplVoc of ~670 mV are comparable or even slightly better than the reports on passivation of n+ surfaces by AlOx layers obtained by plasma assisted ALD [21] and PECVD SiOx2/ALD AlOx or wet chemical SiOx/ALD AlOx [22]. For those schemes a negative fixed charge can be expected. The high level of passivation similar to the performance with neutral fixed charge suggests lower sensitivity to the field effect passivation for the investigated BSF. This implies that the BSF can be improved further towards lower doping levels in order to reduce the impact of the doping-related recombination mechanisms. However such optimization should be compatible with the BSF-functionality and contactability of the n$^+$-surface.

Using various PECVD-SiNx layers from different industrial suppliers on top of NAOS-coated BSF also resulted in functional BSF passivation with J_0 of (105 ± 15) fA/cm^2 and ImplVoc of ~(670 ± 2)mV. In another passivation scheme the NAOS layer in the dielectric

stack was exchanged by ETP PECVD-SiOx (SiOx2-SiNx3) yielding comparable J_0 values and thereby compatible with the set target for highly efficient cells. This result was retained even for reduced thickness of the ETP PECVD-SiOx (SiOx2-thin-SiNx3). In the latter cases the passivation mechanism may combine both chemical and field effect functionalities, however it is less effective compared to the chemical passivation supplied by AlOx deposited on NAOS or ALD SiOx.
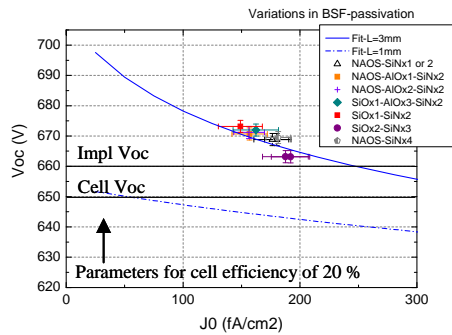
Figure 5: Model calculations of the dependence of Voc on recombination current J_0 for two typical minority carrier diffusion lengths, L in the n-type base of 1 and 3 mm. The experimental results for the phosphorous BSF passivation schemes are also shown in the graph

Similar to the boron emitter passivation performance described in the previous section, the BSF results are also well compatible with the numerical calculations for higher quality n-type material with diffusion length 3 mm (Figure 5).

Comparing the results of sections 3.1 and 3.2 on p+ emitter and n+ BSF samples, we find that with NAOS-AlOx-SiNx samples iVoc values above 670 mV can be obtained for both emitter and BSF doping. Also the ALD SiOx-AlOx-SiNx layer provides excellent passivation on both surfaces.

4 SUMMARY AND CONCLUSIONS

We performed a direct comparison of different dielectric layers and stacks on the passivation properties of boron doped p++-emitters and phosphorous doped n+-BSF prepared using industrial BBr3 or POCl3 tube furnace diffusion processes. The investigated passivation schemes were obtained using various deposition technologies comprising industrial PECVD systems and/or ALD both in industrial and lab scale configurations. All layers described in this paper are in principle suitable to passivate >20% n-Pasha solar cells.

In case of p++-emitter the best results were achieved by combining chemical and field effect passivation using stacks with wet chemical oxide/ALD-AlOx capped with PECVD-SiNx. This passivation scheme yielded iVoc of (673 ± 2) mV and J_0/side after correction for the texture of (40 ± 2) fA/cm^2. The applied ALD-AlOx layers in this case were deposited by two novel industrial scale tools: temporal, low pressure ALD, batch system and spatial, atmospheric pressure ALD, which performed equally successful in our study.

In case of n+ BSF the best performing layer has a 0

fixed charge and thus relies solely on chemical passivation to reduce the D_{it}. Values for iVoc of (673 ± 2) mV and J_0/side after correction for the texture of (80 ± 2) fA/cm^2 were found. Also the industrial ALD-Alox layers performed very well, yielding only slightly lower values for iVoc.

Combining the results for both p+ and n+ areas, we find that a highly functional passivation scheme can be realized suitable for both p++ and n+ diffused fields. Using NAOS-ALOx-SiNx or SiOx-AlOx-SiNx passivation on both emitter and BSF side, n-Pasha cells yielding > 20% cell efficiency can be obtained, while this also offers the possibility for transfer this passivation scheme to advanced cell architectures such as IBC.

REFERENCES

[1]   International technology roadmapfor photovoltaic (ITRVP), in 2012.
[2]   Yingli press release, in 2010.
[3]   A.R. e. al. Burgers, 19% efficient n-type Si solar cells made in pilot production, 2010.
[4]   D.M. Powell, M.T. Winkler, H.J. Choi, C.B. Simmons, D. Berney Needleman, T. Buonassisi, Energy and Environmental Science, 2012, 5874.
[5]   L.J. Geerligs, N. Guillevin, I.G. Romijn, Photovoltaics International, 2011, 94.
[6]   I.G Romijn, Gutjahr A., Saynova D., Anker J., Kossen E., Tool C.J.J, Photovoltaics International, 2013, 44.
[7]   A.G. Aberle, Progress in Photovoltaics, 2000, *8*, 473.
[8]   G. Dingemans, N.M. Terlinden, M.C.M. Verheijen, M.C.M. van de Sanden, W.M.M. Kessels, Journal of Applied Physics, 2011, *110*, 093715.
[9]   V.D. Mihailetchi, Y. Komatsu, L.J. Geerligs, Applied Physics Letters, 2008, *92*, 63510.
[10] J. Benick, B. Hoex, M.C.M. van de Sanden, W.M.M. Kessels, O. Schultz, S.W. Glunz, Applied Physics Letters, 2008, *92*, 53504.
[11] J. Benick, A. Richter, M. Hermle, S.W. Glunz, Physica Status Solidi-Rapid Research Letters, 2009, *3*, 233.
[12] B. Hoex, J. Schmidt, R. Bock, P.P. Altermatt, M.C.M. van de Sanden, W.M.M. Kessels, Applied Physics Letters, 2007, *91*, 12107.
[13] G. Dingemans, E. Kessels, Journal of Vacuum Science & Technology A, 2012, *30*, 40802.
[14] B. Hoex, J. Schmidt, P. Pohl, M.C.M. van de Sanden, W.M.M. Kessels, Journal of Applied Physics, 2008, *104*, 44903.
[15] G. Dingemans, C.A.A. van Helvoirt, D. Pierreux, W. Keuning, W.M.M. Kessels, Journal of the Electrochemical Society, 2012, *159*, H277-H285.
[16] A. Cuevas, R.A. Sinton, M. Kerr, D. Macdonald, H. Mackel, Solar Energy Materials and Solar Cells, 2002, *71*, 295.
[17] D.E. Kane, R.M. Swanson, Measurement of the emitter saturation current by a contactless photoconductivity decay method, presented at *IEEE Photovoltaic Specialists Conference*, 1985.
[18] P. Saint-Cast, D. Kania, R. Heller, S. Kuehnhold, M. Hofmann, J. Rentsch, R. Preu, Applied Surface Science, 2012, *258*, 8371.
[19] A. Richter, J. Benick, M. Hermle, Ieee Journal of Photovoltaics, 2013, *3*, 236.

[20] Romijn I.G., L. Fang, A. Vlooswijk, Photovoltaics International, 2012, 63.
[21] B. Hoex, M.C.M. van de Sanden, J. Schmidt, R. Brendel, W.M.M. Kessels, Physica Status Solidi-Rapid Research Letters, 2012, *6*, 4.
[22] S. Bordihn, G. Dingemans, V. Mertens, J.W. Muller, W.M.M. Kessels, Ieee Journal of Photovoltaics, 2013, *3*, 925.